Chaos, Solitons and Fractals 188 (2024) 115566

Contents lists available at ScienceDirect

Chaos, Solitons and Fractals

journal homepage: www.elsevier.com/locate/chaos

Disruptions in segregation mechanisms in fMRI-based brain functional network predict the major depressive disorder condition

Vladimir S. Khorev [a,b], Semen A. Kurkin [a], Gabriella Zlateva [c], Rositsa Paunova [c], Sevdalina Kandilarova [c], Michael Maes [c], Drozdstoy Stoyanov [c], Alexander E. Hramov [a,*]

[a] Baltic Center for Neurotechnology and Artificial Intelligence, Immanuel Kant Baltic Federal University, 14 A. Nevskogo ul., Kaliningrad, 236016, Russia
[b] Neuroscience and Cognitive Technology Lab, Innopolis University, 1 Universitetskaya Str., Innopolis, 420500, Russia
[c] Research Institute, Department of Psychiatry and Medical Psychology, Medical University Plovdiv, 15A Vassil Aprilov Blvd., Plovdiv, 4002, Bulgaria

ARTICLE INFO

Keywords:
fMRI
Network analysis
Consensus networks
MDD
Healthy controls
Classification

ABSTRACT

This study investigates the functional brain network in major depressive disorder using network theory and a consensus network approach. At the macroscopic level, we found significant differences in connectivity measures such as node strength and clustering coefficient, with healthy controls exhibiting higher values. This is consistent with disruptions in functional brain network segregation in patients with major depressive disorder. Consensus network analysis revealed that the central executive and salience networks were predominant in healthy controls, whereas depressed patients showed greater overlap with the default mode network. No differences were found in network efficiency measures, indicating comparable brain network integration between healthy controls and major depressive disorder groups. Importantly, the clustering coefficient emerged as an effective diagnostic biomarker for depression, achieving high sensitivity (90%), specificity (92%), and overall precision (90%). Further analysis at the mesoscale level uncovered unique functional connections distinguishing healthy controls and major depressive disorder groups. Our findings underscore the utility of analyzing functional networks from the macroscale to the mesoscale, and provide insight into overcoming the challenges associated with intersubject variability and the multiple comparisons problem in network analysis.

1. Introduction

The integration of the concept of brain functional networks [1,2] and the theory of complex networks [3,4] provides a powerful tool for studying brain processes in both healthy individuals and those with various pathologies [5,6]. A brain functional connectivity network describes statistical associations of neural activities between distinct and distant brain regions [7]. However, the intrinsic properties of brain functional networks complicate their application and analysis using conventional statistical and machine learning approaches.

The first challenge is the large feature space at the level of a brain functional network (e.g., for 165 brain regions, there are 13530 unique connections, as well as various network measures, both global and local). Consequently, there is a problem of detecting spurious correlations and significant effects; in statistics, this is called the multiple comparisons problem [8].

The second challenge is the high level of inter-subject variability, i.e., variability in the characteristics of brain functional networks across individuals in the same group. Many factors contribute to intersubject variability, including genetics, gender, age, health status, cognitive level, and other exogenous and endogenous factors. Regardless of the cause, this problem makes it difficult to identify robust biomarkers of brain states, including those that reflect the development of pathological processes from the point of view of functional connectivity.

One possible way to address the first challenge is to reduce the feature space by using network measures instead of individual connections and by constructing higher-level features. This corresponds to the transition from mesoscale (the level of individual brain regions and connections) to macroscale (the level of subnetworks/clusters and global networks) analysis of the brain network [9–11]. In particular, it allows one to analyze the properties of the brain functional network from the perspective of considering the processes of integration and segregation.

Integration and segregation are key concepts in understanding how functional brain networks operate, describing how different regions of the brain interact and process information to produce coordinated

* Corresponding author.
E-mail address: aekhramov@kantiana.ru (A.E. Hramov).

https://doi.org/10.1016/j.chaos.2024.115566
Received 20 August 2024; Accepted 19 September 2024
Available online 1 October 2024
0960-0779/© 2024 Elsevier Ltd. All rights are reserved, including those for text and data mining, AI training, and similar technologies.

cognitive functions [12,13]. Integration refers to the process by which different brain regions or subnetworks work together to produce a unified response or behavior. It involves the cooperation of multiple, often distant, brain regions, allowing information from different sources to be combined into a coherent whole. This is critical for complex cognitive tasks that require the coordination of different types of information, such as perception, attention, and memory. Segregation refers to the process by which different regions of the brain specialize and operate relatively independently to perform specific functions. It involves the organization of the brain into distinct modules or communities, each responsible for a particular type of information processing. The functional network of the healthy brain operates on a delicate balance between integration and segregation [14].

The high level of inter-subject variability can be overcome by identifying a group-specific functional network. The analysis is then performed on such a network, rather than on the networks of individual subjects. This approach, called consensus network analysis, was developed in relation to fMRI-based functional brain networks in Ref. [15].

In this paper, we utilized the above two techniques to address the challenging task of detecting macroscale disruptions in the functional brain network associated with the presence of major depressive disorder (MDD) in a patient and identifying robust biomarkers of the disease.

Mental disorders in general appear to be one of the determinants of the world-wide burden of global disability — adjusted years [16,17]. MDD is one of the main causes of disability worldwide and is characterized by symptoms like fatigue, insomnia, and loss of appetite. Anhedonia is one of the key symptoms in the disorder and often it is accompanied by cognitive impairments and suicidal thoughts [18]. The percentage of people diagnosed with depression increases every year. About 300 million people in the world are affected by the condition, which makes it one of the main causes of disability. According to WHO, it is predicted by 2030 MDD to ranked first in terms of disease of burden [19]. Pharmacological treatment can influence some of the symptoms during the episodes, however patients may experience recurrence within a short time after discontinuing medication [20]. Moreover, the outcome of therapeutic strategies is suboptimal given that roughly 50% of patients do not adequately respond to antidepressants [21,22].

Despite decades of research demonstrating alteration in various biological systems, the underlying mechanisms of MDD are still not fully understood [23]. MDD has been associated with alterations in structure and function of the brain [24], immunological changes [25], neurotransmitters [26], neurotrophic factors [27], and oxidative stress [28] . Finding objective biomarkers have been critical challenge in the psychiatric field where the current diagnostic process is based on subjective assessments of patient's narratives, as the current diagnostic procedures are based exclusively on interviews/ rating scales [29].

Resting state functional magnetic resonance imaging (rs-fMRI) is a promising technique allowing for the investigation of changes in interregional connectivity [30]. The science of large-scale neural networks provides a robust model for characterizing the neurobiology of psychiatric conditions [31]. This model emphasizes the importance of several global networks that perform different roles in human cognition by mapping salient external and internal events – the Salience network (SN), executing cognitive control – the Central Executive Network (CEN) and the Default Mode Network (DMN), the activity of which increases during rest and decreases during task performance [32,33].

During resting state there have been reported a number of alterations in brain effective and functional connectivity [34,35]. Researchers found altered effective connectivity among the cerebellum and cerebrum during resting-state and implicate the finding as potential biomarker for depressive disorder [36]. Also, there are increased connections from cerebellum to right thalamus and decreased connections from the cerebellum to right angular gyrus and right precuneus [37]. Abnormalities in DMN and Limbic network were found in patients with depression, compared to patients with bipolar disorder [38] Moreover, there is enhanced functional connectivity between the thalamus and somatosensory cortex in patients with MDD, compared with healthy controls [39]. Metaanalisis data suggests that MDD is characterized by hypoconnectivity within the frontoparietal network and dorsal attention network, and between emotion and SN, and hyperconnectivity within the DMN [40,41].

All the above research maps the findings onto established global connectivity networks. In our previous research, we have explored the potential of connectivity measures which identified patterns during rs-fMRI in a sample of MDD patients and were able to identify the main hubs common for network measures such as node strength and clustering coefficient (lingual gyrus, superior occipital gyrus, and middle occipital gyrus) [42]. Moreover, good classification accuracy (area under the curve — 0.92) was achieved by using the full connectivity matrices. In recent studies, we have also considered MDD classification using both deep learning methods based on graph neural networks [43], which have been used to classify topological features of functional brain networks, and interpretive machine learning methods [44], which have used various global network measures (clustering coefficient, small-world coefficient, shortest path).

2. Subjects and methods

2.1. Subjects

We enrolled a total of 164 participants, comprising 94 individuals without any known psychiatric conditions (Healthy Controls, HC group) and 70 patients experiencing with major depressive disorder (MDD group). Each participant underwent thorough evaluations conducted by experienced psychiatrists, including the administration of the Mini International Neuropsychiatric Interview [45] and the Montgomery–Åsberg Depression Rating Scale (MADRS) [46,47]. Exclusion criteria for both groups included a history of comorbid psychiatric conditions, autoimmune diseases, neurological disorders, previous head trauma, or the presence of metal implants incompatible with MRI scans. Prior to participation, all individuals provided written consent in accordance with the principles outlined in the Declaration of Helsinki. The study protocol was reviewed and approved by the Ethical Committee of the Medical University of Plovdiv (Approval No: 2/19.04.2018).

There were no significant differences between the two groups in terms of mean age, sex distribution, or level of education. However, as anticipated, patients exhibited significantly higher MADRS scores compared to the healthy controls (see Table 1).

2.2. MR scanning and image processing

The MR scanning procedure was performed on a 3T MRI system (GE Discovery 750w). The protocol included a high-resolution structural scan (Sag 3D T1) with slice thickness of 1 mm, matrix 256 × 256, TR (relaxation time) 7.2 s, TE (echo time) 2.3 s, and flip angle 12°, FOV 24, resting-state functional scan — with slice thickness 3 mm, matrix 64 × 64, repetition time — 2000 ms, echo time — 30 ms, flip angle 90°, 192 volumes [48].

Neuroimaging data were processed using SPM 12 software (Statistical Parametric Mapping, http://www.fil.ion.ucl.ac.uk/spm/). The functional images of each participant were first realigned, co-registered with the high-resolution anatomical image, and normalized to standard MNI space. Parameters for the realignment step were the following: quality 0.9, separation 4, no smoothing, 2-nd degree B-spline interpolation, no wrap, 12 × 12 basis function, regularization 1 with medium factor, without Jacobian deformations, 5 iterations, average Taylor expansion point. Additionally, the program's default pipeline incorporated a motion-correction step for each patient. The co-registration

Table 1
Demographic and clinical characteristics of the groups.

	Healthy controls (n=94)	Patients (n=70)	Significance
Age (mean ± SD)	40.6 ± 11.8	41.0 ± 13.2	0.961[a]
Sex (M/F)	41/53	27/44	0.996[b]
Education (secondary/higher)	6/89	7/63	> 0.999[b]
MADRS score (mean ± SD)	2.0 ± 2.6	29.5 ± 6.0	< 0.001[a]

SD — Standard Deviation.
[a] Two-sample Kolmogorov–Smirnov nonparametric test.
[b] χ^2-test, MADRS — Montgomery–Åsberg Depression Rating Scale.

method was set to the normalized mutual information with the following parameters: separation [4 2], tolerances [0.02 0.02 0.02 0.001 0.001 0.001 0.01 0.01 0.01 0.001 0.001 0.001], histogram smoothing [7 7]. MNI normalization parameters were the following: bias regularization 0.0001, bias FWHM 60 mm cutoff, affine regularization ICBM European brain template, warping regularization [0 0.001 0.5 0.05 0.2], no smoothing, sampling distance 3.

As a result, we obtained voxel-level blood-oxygen-level-dependent (BOLD) signals.

2.3. Network analysis

2.3.1. Reconstruction of brain functional network

The brain volume was parcellated into 165 regions (see Supplementary material S1) according to the automated anatomical labeling atlas AAL3 [49]. We have chosen the AAL atlas because of its widespread use in functional network analysis [50]. To assess the connectivity between pairs of brain regions (the so-called, connectivity matrix), we calculated the average BOLD time series $x_i(t)$ for each of 165 brain parcellations (nodes), detrended them, and estimated Pearson correlation coefficients r for all pairs of the averaged parcellation activities [51]. The resulting connectivity matrix represents the functional brain network.

2.3.2. Network measures

To analyze the topology and macroscale properties of a functional network, we considered the following network measures: node strength, betweenness centrality, eigenvector centrality, clustering coefficient (CC), global and local efficiency. We computed both the distribution of these metrics across nodes and the network-wide averages (except for global efficiency, which is by definition a network-wide measure). These metrics provide valuable insights into the connectivity patterns and the characteristics of segregation and integration of brain networks:

- The node strength determines how strongly a node is directly connected to other nodes in the network by summing the absolute edge weights associated with the edges connected to it. All values are standardized and higher values indicate higher centrality within the network [52].
- The betweenness centrality represents the fraction of all shortest paths within the network that pass through the given node. Nodes with higher betweenness values share a large number of shortest paths [53]. This metric has been shown to be useful in detecting traumatic brain injury [54].
- Eigenvector centrality is a self-referential importance metric: nodes have an increased importance value if they are connected to other important nodes. The eigenvector centrality of a node i is equal to the ith element of the eigenvector related to the largest eigenvalue of the adjacency matrix [55].
- The clustering coefficient assesses the amount of connectivity between neighboring nodes in the network. The weighted clustering coefficient calculates the average intensity of all triangles associated with each node [56].
- The path length metric reflects the average shortest path length in the network. The global efficiency metric is the average of the inverse of the shortest path [57]. The local efficiency metric is essentially the global efficiency calculated based on the neighbors of a given node. In neuroscience, efficiency is used to discuss data transfer through a neural network.

2.3.3. Consensus network

To reduce intersubject variability, we used the concept of consensus network which was first proposed for fMRI-based functional network in the Ref. [15]. The basic idea behind constructing a consensus network is to identify the common connections observed in the majority of networks within each group (HC and MDD groups). To determine the consensus network, we first removed all insignificant connections (with $p > 0.05$) and then kept only those connections that were present in all subjects of the respective group (HC or MDD). Algorithmically, to construct a consensus network, we perform the following procedure for each group:

1. Binarization of all networks based on the significance levels p, so that each connection strength w_{ij} between nodes i and j is transformed as:
$$w_{ij} = \begin{cases} 1, p_{ij} < 0.05 \\ 0, p_{ij} \geq 0.05. \end{cases} \quad (1)$$
2. Averaging of binarized connection strengths over all networks in the group:
$$w^*_{ij} = \frac{1}{N} \sum_{n=1}^{N} w^n_{ij}, \quad (2)$$
where n is the network number, N is the number of networks in the group.
3. Binarization of the resulting connection strengths as follows:
$$\tilde{w}_{ij} = \begin{cases} 1, w^*_{ij} \geq 0.99 \\ 0, w^*_{ij} < 0.99. \end{cases} \quad (3)$$
The resulting connectivity matrix $\tilde{\mathbf{w}}$ corresponds to the consensus network for the considered group.

2.3.4. Optimal community structure

We determined the optimal community structure that represents a subdivision of the network into distinct groups of nodes (called clusters or modules), which maximizes the number of edges between members within each subgroup and minimizes the number of edges between subgroups [58]. We did not use any initial community affiliation vector and used the Louvain community detection algorithm with the resolution parameter was set to 0.05, objective function type or custom objective matrix was set to symmetric treatment of negative weights.

For the network calculations we used the Brain Connectivity Toolbox [59].

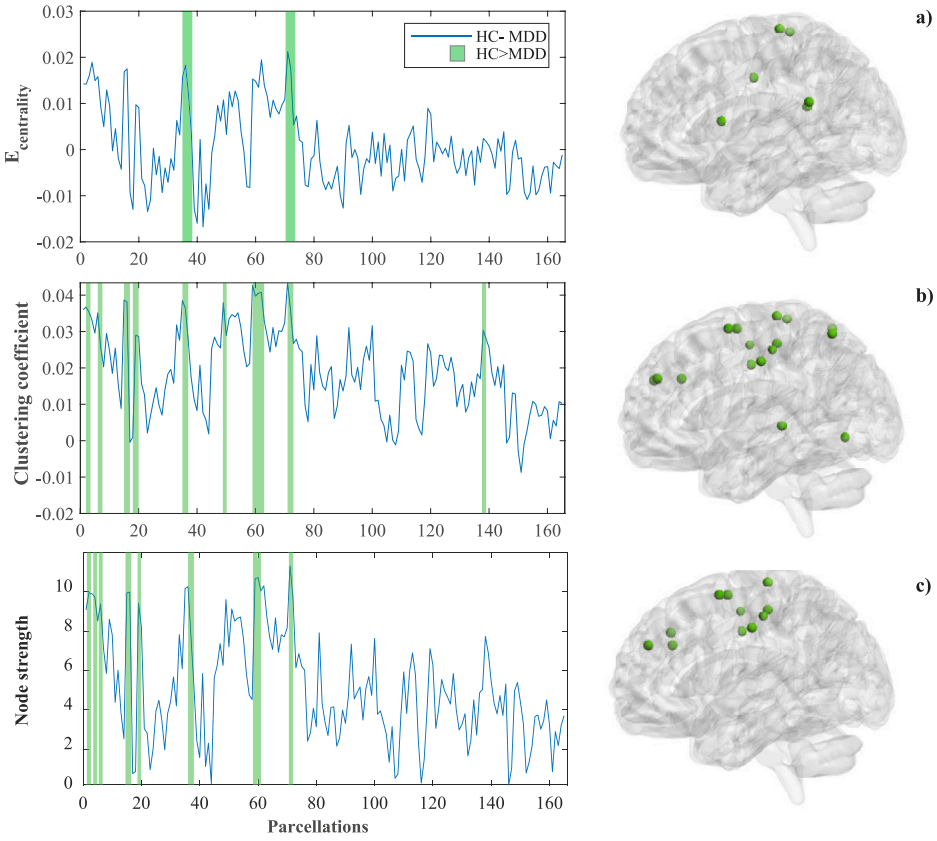

Fig. 1. (Left panel) The distributions across nodes of the differences between the group-averaged network measures for the HC and MDD groups for (a) eigenvector centrality, (b) clustering coefficient and (c) node strength. The green shaded intervals indicate the node numbers for which the corresponding network measure is significantly higher in the HC group compared to the MDD group. Statistical inferences were made using permutation tests with Bonferroni correction. (Right panel) The brain images with the significant nodes from the corresponding left panels.

2.4. Statistical analysis

2.4.1. Comparison of mean measures

To identify significant differences in the averaged network measures at the group level (HC vs. MDD), we performed statistical tests separately for each measure using the t-test. We used the Kolmogorov–Smirnov one-sample test to test the normality of the distributions.

2.4.2. Comparison of distributions of network measures

To address the multiple comparisons problem and a possible non-normality of the distributions of network measures across nodes, we used the following permutation-based approach with the Bonferroni correction for 165 comparisons for individual regions. First, for each node, we computed the difference between the group-averaged network measures for the initial HC and MDD groups. Next, the samples from the MDD and HC groups were pooled, and the differences between the group-averaged network measures were computed for different ways of dividing the pooled values into two groups of size HC and MDD. The set of these computed measures was the possible distribution for this sample under the null hypothesis that the group labels were interchangeable (i.e., randomly assigned). After 10000 permutations, we obtained the permutation distribution for each node. We could then determine the position of the initial difference value on the permutation distribution. If it was within the Bonferroni-corrected 95th percentile (or 97.5th percentile for the two-tailed test), the null hypothesis was true, otherwise it was rejected.

2.5. Linear discriminant analysis

We utilized Linear Discriminant Analysis (LDA in Classification learner toolbox, Matlab) to explore the accuracy of diagnosis classification based on different network features. The linear coefficient threshold was set to zero. The discriminant type was set to the recommended by the toolbox "pseudolinear" or "pseudoquadratic" type to avoid problems with zeroes and negative values in the predictors set. Other parameters including the enforced amount of regularization or prior probabilities were not applied. The chance level of the LDA for the considered problem is 50%.

We denoted true positive as TP, false positives as FP, and negatives as TN and FN. Then, the precision of the model was calculated as

$$\text{Precision} = \frac{TP}{TP + FP},$$

specificity as

$$\text{Specificity} = \frac{TN}{TN + FP},$$

sensitivity as

$$\text{Sensitivity} = \frac{TP}{TP + FN},$$

and F1-score as

$$F1 = \frac{2 * \text{Precision} * \text{Sensitivity}}{\text{Precision} + \text{Sensitivity}}.$$

2.5.1. K-fold cross-validation

LDA k-fold cross-validation is a machine learning technique that evaluates the predictive power of a model by dividing the dataset into multiple subsets (called folds), training the model on the subsets, and validating it on the remaining fold. This approach improves the accuracy of the evaluation by ensuring that it is performed on the unseen data. It also helps avoid the problem of potential overfitting, where a model is too specific to the training data. Using k-fold cross-validation with $k = 5$ in our work meant dividing the dataset into 5

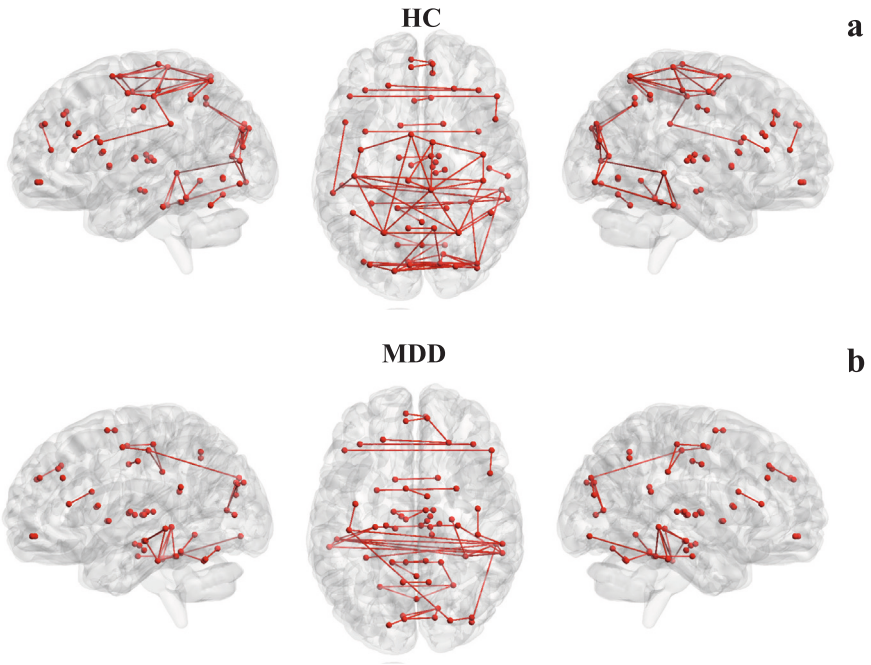

Fig. 2. (A) Group-averaged connectivity matrices for the HC and MDD groups. (B) Matrices corresponding to the calculated consensus networks for the HC and MDD groups.

folds, training the model on 4 folds (80% of the data), and validating it on the remaining fold (20% of the data). This process was then repeated 5 times, with the validation data changing in each iteration. The average accuracy across all iterations was used to evaluate the performance of the model. To further reduce overfitting and variance in the results and to provide a more accurate and robust assessment of the model's predictive power, we repeated the entire process of dividing the dataset into 5 folds, training the model on 4 folds, and validating it on the remaining fold 100 times, and calculated the average.

2.6. Correspondence to the large-scale brain networks

To determine the similarity of the considered subnetwork to the large-scale brain network, we calculated the ratio of common nodes between these networks to the total number of nodes in the large-scale network. This resulted in the percentage of similarity of the considered subnetwork to the large-scale brain network. The composition of nodes (brain regions) included in large-scale brain networks was determined based on the literature review [60–62]. We considered the following major large-scale brain networks: Default Mode Network (DMN), Central Executive Network (CEN), Left Ventral CEN (LCEN), Right Ventral CEN (RCEN), Dorsal CEN (DCEN), Dorsal Attention Network (DAN), and Salience Network (SN); the lists of nodes for these large-scale networks are shown in Supplementary Material S2.

3. Results

3.1. Network measures analysis

The character group-averaged connectivity matrices for the HC and MDD groups are shown in Fig. 2A. Qualitatively (visually) these matrices are very similar. Nevertheless, t-test revealed that the network-wide averaged node strength and clustering coefficient are significantly higher in the HC group compared to the MDD group (see Table 2).

The permutation test found the sets of nodes where the local network measures differed significantly between the HC and MDD groups (see Fig. 1). The largest set of significant nodes is observed for clustering coefficient and the smallest set was found for eigenvector centrality; significant nodes were also found for node strength. There were significant effects only in one direction (HC>MDD). There were no significant effects for betweenness centrality, local and global efficiency.

Table 2
Statistical effects of different global network measures.

Measures	T_{162} HC>MDD	p
Eigenvector centrality	0.9795	0.3288
Node strength	14.8127	<0.0001
Clustering coefficient	21.2212	<0.0001
Betweenness centrality	−0.1606	0.8726
Global efficiency	1.4545	0.1477
Local efficiency	−0.8350	0.4049

A higher clustering coefficient reflects a higher level of segregation within local clusters in healthy controls, indicating that information is processed efficiently within localized brain subnetworks or clusters [63]. Moreover, the significant effect for the corresponding average metric (Table 2) means that the higher level of segregation in the HC group is observed in most brain regions. The effects found for the node strength (Fig. 1c and Table 2) are consistent with the above conclusion. At the same time, the lack of statistical effects for global efficiency means that global integration processes in the brain do not differ significantly between the HC and MDD groups, suggesting that information transfer between network clusters is not fundamentally different between the groups.

Interestingly, the significant nodes for eigenvector centrality, where values are higher in the HC group, are mainly located in the cerebral cortex (Fig. 1a). A high eigenvector centrality means that the node is connected to a high number of important or hub nodes [64]. Thus, we identified disparities in the localization of important hubs in the HC and MDD groups.

3.2. Analysis of consensus networks

We calculated consensus networks for the HC and MDD groups (see Figs. 2B and 3) to identify differences between the groups in specific network patterns. The consensus networks show clearly distinguishable differences between the HC and MDD groups. We compared these

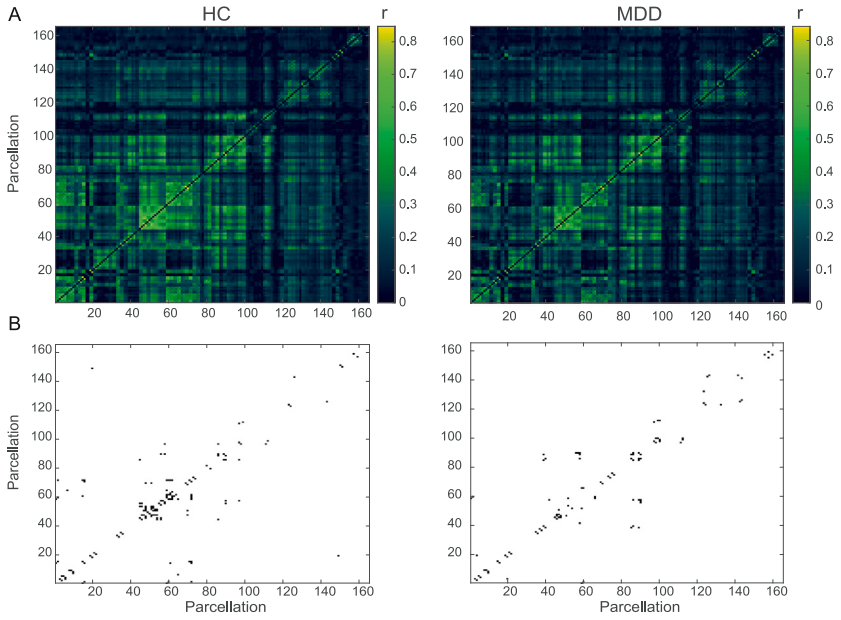

Fig. 3. Consensus networks for the (a) HC and (b) MDD groups. Dots represent nodes in the network, while straight lines depict the connections between them.

Table 3
Correspondence of the consensus networks of the HC and MDD groups to the large-scale brain networks; the table shows the correspondence percentages, the number of matching nodes to the total number of nodes for each large-scale network.

Consensus network	DMN	CEN	LCEN	RCEN	DCEN	DAN	SN
HC group	60% 6/10	80% 8/10	83% 5/6	60% 3/5	92% 11/12	17% 2/12	100% 6/6
MDD group	80% 8/10	50% 5/10	67% 4/6	60% 3/5	83% 10/12	17% 2/12	33% 2/6

DMN (Default mode network), CEN (Central executive network),
LCEN (Left Ventral CEN), RCEN (Right Ventral CEN), DCEN (Dorsal CEN),
DAN (Dorsal attention network), SN (Salience network).

networks at the macroscale level by analyzing differences in the their correspondence to large-scale brain networks (see Table 3).

We can speculate that the more pronounced overlap with a large-scale network in the control group indicates the hypoactivity of this network in MDD patients. On the other hand, the prevalence of overlap in the MDD group is not normal and indicates hyperactivity or compensatory activity. Table 3 shows that CEN and SN predominate in the HC group, while the MDD consensus network has more overlap with the DMN, which is responsible for internally oriented attention and self-referencing [65].

3.3. Analysis of optimal community structure

The results of Section 3.1 indicated differences in clustering processes between the HC and MDD groups. For a more detailed analysis, in this section we investigate the distinctions in emerging clusters at the mesoscale level by detecting optimal community structures in the consensus networks.

17 non-overlapping communities (clusters) were obtained for the HC group and 19 — for the MDD group. However, most of them contain 2–3 connections, so we left only relatively large communities with 5 or more connections. This resulted in three communities each for both the HC and MDD groups (see Fig. 4 and Supplementary Material S3 for details). One can see that the identified clusters differ both in size (the clusters in the HC group are significantly larger) and in their constituent connections. To analyze the differences in clustering between groups at the level of individual connections, we generated Fig. 5. Here, in the circulograms, the color indicates the common and unique connections for the groups for each of the 3 clusters considered (Supplementary Material S3 details these connections).

Fig. 5 shows that clusters 1 and 3 are significantly larger in the HC group, while cluster 2 is about the same size in the MDD and HC groups; however, the composition of connections for this cluster differs significantly between the groups. Although it is located in occipital and temporal regions in both groups, it contains more connections from the limbic system of the brain and the cerebellum in the MDD group. We can also see that the MDD group has the most disruptions in the connections of cluster 1. All of the cluster-level effects described above are reflected in the statistical differences found in the network measures (Section 3.1).

3.4. Linear discriminant analysis

We employed linear discriminant analysis (LDA) to investigate the diagnostic power of different network measures (see Table 4). Node-wise clustering coefficient and full functional connectivity matrices show the best classification abilities. This result confirms that the main differences in functional networks between groups are observed in the degree of network segregation. This suggests that the clustering coefficient is an effective biomarker for MDD. Note that even the global clustering coefficient averaged over the whole network has a good classification power.

4. Discussion

The present study has provided some interesting insights into neural connectivity patterns associated with MDD. First, we were able to find significant differences in connectivity measures such as node strength and clustering coefficient (both higher in HC). Notably, the original average correlation matrices are almost indistinguishable between groups (see Fig. 2A). The proposed pipeline based on consensus networks and analysis of macroscopic network characteristics allows us to distinguish and highlight subtle differences in the organization of brain networks caused by the development of MDD (see, e.g., Fig. 2B, which shows consensus networks with clearly visible differences between HC and MDD groups).

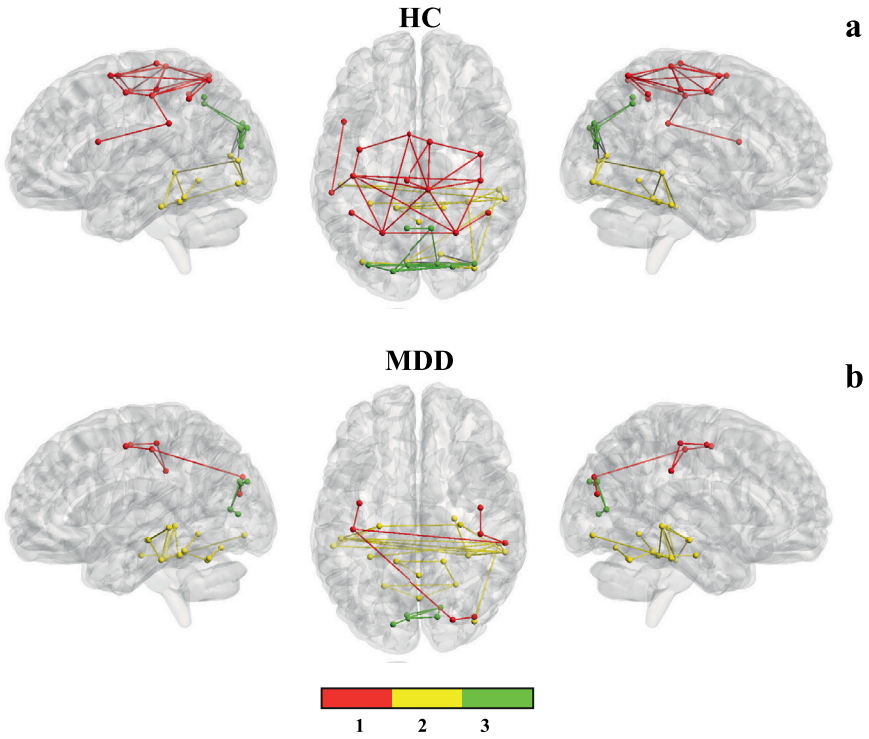

Fig. 4. Three largest non-overlapping optimal communities (clusters) for (a) HC and (b) MDD groups. The color indicates different clusters and their constituent connections. Dots represent nodes in the network, while straight lines depict the connections between them.

Table 4
Classification accuracy with different network measures as features.

Feature vector	Accuracy (Mean ± SD)	Sensitivity	Specificity	Precision	$F1$
Full functional connectivity matrices	0.9195 ± 0.1039	88%	93%	91%	0.89
Node-wise clustering coefficient	0.8762 ± 0.0194	90%	92%	90%	0.90
Global Clustering coefficient	0.77439 ± 0.1510	88%	79%	70%	0.77
Node-wise node strength	0.6158 ± 0.0306	54%	67%	57%	0.55
Node-wise eigenvector centrality	0.4602 ± 0.0255	50%	52%	39%	0.43
Node-wise betweenness centrality	0.5354 ± 0.0324	45%	61%	57%	0.50
Local efficiency	0.4751 ± 0.0196	44%	41%	34%	0.38
Global efficiency	0.7926 ± 0.0085	75%	83%	78%	0.76

Next, the analysis of the consensus networks demonstrated that HC prevails in CEN and SN, while MDD has bigger overlap with DMN. Finally, clustering coefficient was identified as the most suitable measure for classification purposes reaching 90% sensitivity, 92% specificity and 90% overall precision. The significance of these findings will be discussed in the following lines.

Decreased node strength is a common observation for patients suffering from depression, although literature on the topic is limited. In a study by Jacob et al. [66] using fMRI-based functional networks, they reported reduced node strength of the right precuneus, a key region within the DMN, which correlated negatively with higher levels of maladaptive rumination in MDD patients. Further evidence confirming the relevance of node strength in understanding MDD, is given by Huang et al. in their recent article highlighting changes in the delta wave activity measured through EEG [67]. The authors noted decreased mean node strength and clustering coefficient in MDD patients, and in addition improvement following antidepressant therapy was also reported.

Despite the methodological variance, the findings align with our results on the impact of depression on neural connectivity. Jacob et al. [68] also acquired similar results using a different method — diffusion MRI. The findings demonstrated decreased node strength in critical areas such as the right hippocampus, right pallidum, and left precentral and postcentral gyri in MDD patients.

On the other hand, the study of Liu et al. [69] revealed increased node degree in the right amygdala and putamen in MDD patients, which is divergent from our findings. However, the key distinction from our study is that node degree only measures the quantity of connections, while in calculating node strength, the intensity of the connections is also considered. This suggests that while node degree was increased, it does not necessarily reflect the functional efficacy or intensity of neural connections.

Clustering coefficient, just like node strength, was significantly lower in the patients we studied aligning with findings from Xia et al. [70] and Wu et al. [71]. Wu et al. focused their research on drug-naive adolescents with a first episode of MDD, which accentuates clustering coefficient's potential as an early diagnostic biomarker. Borchardt et al. [72] also observed decreased global clustering coefficient, indicating less network segregation.

Contrarily, some studies failed to detect significant differences in the clustering coefficient of MDD patients compared to HC [73,74]. The discrepancies might be attributed to the small size and heterogeneity of the samples, and varied methodologies. In their study, He et al. [75] observed a non-significant decrease in CC among patients with depression; however, when compared to bipolar disorder patients, the difference was actually significant with bipolar disorder patients exhibiting a higher mean value. Thus, we can speculate that measuring clustering coefficient could be potentially used for differential diagnostic purposes as well.

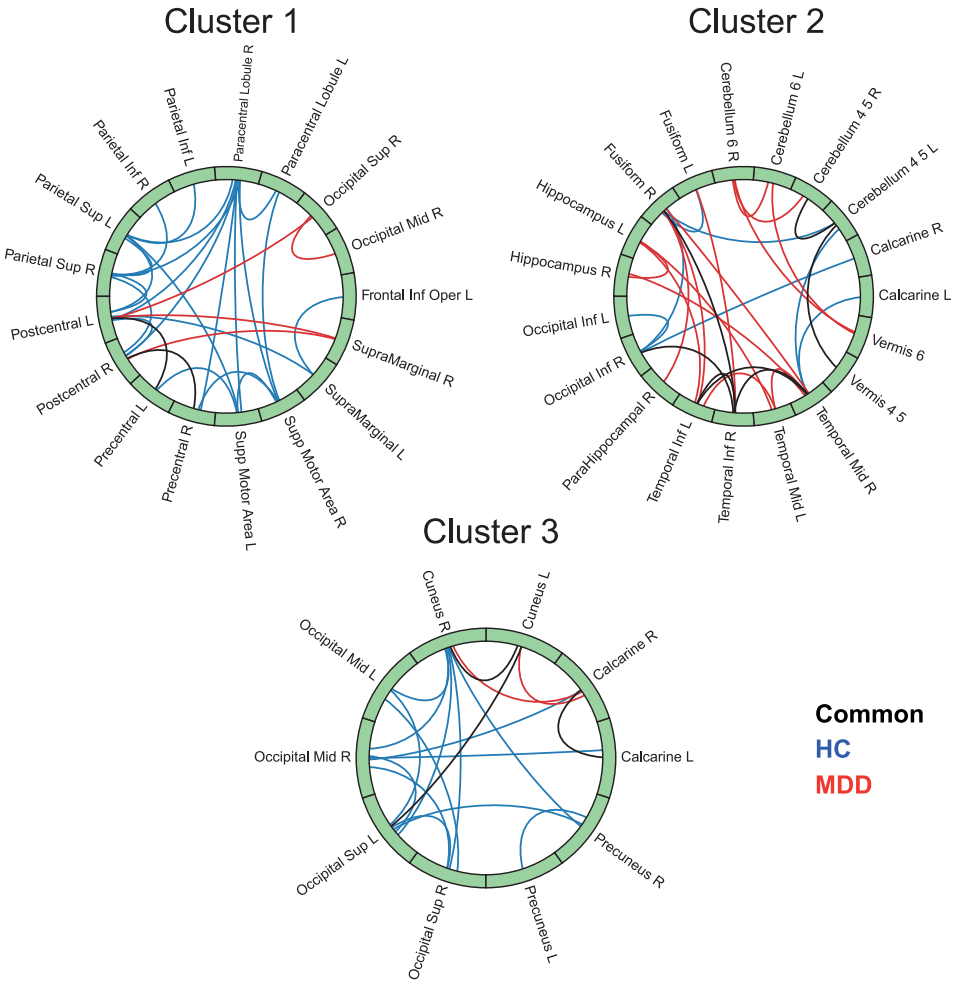

Fig. 5. The circulograms illustrate the 3 largest clusters (see also Fig. 4) and their constituent connections. Here, black color denotes the connections common to the HC and MDD groups, blue color denotes the connections unique to the HC group, and red color denotes the connections unique to the MDD group. Supplementary Material S3 details these connections.

Further support for the potential of clustering coefficient measures as biomarkers is given by studies, which suggest that following antidepressant therapy CC tends to decrease (resulting in reduced local efficiency), while global efficiency may increase [76,77]. This expands the potential utility of CC, as it could be used to monitor the effects of antidepressant medication.

The findings of reduced clustering coefficient and global efficiency suggest that MDD patients' network organization is both less locally specialized and less globally integrated. Our research, on the other hand, did not find any significant difference between the global efficiency of depressed patients and healthy controls. Our interpretation of this result is that the difference exists in segregation, rather than integration. The explanation for these distinctive results could be linked to alternative methodologies, MDD heterogeneity, sample sizes and co-occurring factors, such as stress and anxiety.

It is worth noting that mean clustering coefficient exerted prominent level of significance, but it can also be disproportionally influenced by nodes with exceptionally low or high degrees [59]. We have reached the understanding that simply observing node statistics at face value may not offer a comprehensive approach to uncovering innovative solutions to challenges in psychiatry, such as identifying a reliable biomarker for diagnosing MDD. Thus, we furthered our analysis, using the concept of consensus networks that includes functional connections that are present in the majority of patients or healthy subjects [15].

In our analysis of the consensus networks, HC showed group-specific nodes, typical for the CEN and SN. These networks are typically associated with higher-order cognitive functions and the response to salient stimuli, respectively [78]. Conversely, significant overlap with DMN nodes was observed in the consensus networks specific to MDD patients. The DMN is often involved in self-referential thoughts and rumination, which are common in depressive states. The greater overlap in the DMN in MDD indicates increased activity in this network, probably due to hypercompensation. Increased activity is related to increased connectivity.

Alterations in the FC within these networks, as well as between them, are commonly observed in depressed patients. Meta-analysis of Kaiser et al. revealed for MDD patients reduced connectivity within the CEN, hypoconnectivity between the CEN and dorsal attention network (DAN) and hyperconnectivity within the DMN and between the DMN and CEN [30]. Also in 2015, in their systematic review, Mulders et al. [78] determined increased connectivity within the anterior DMN. These findings resonate with our observations of the correspondence with the large-scale brain networks (see Section 3.2 and Table 3).

While some studies support the notion that DMN connectivity is increased in MDD, research over the recent years has yielded more varied results. In 2019, Yan et al. [79] gathered data from 25 research groups involving 848 MDD patients, and found that there was actually decreased DMN functional connectivity. In the 2020 study by Jacob et al. [66], higher rumination scores in MDD patients (but also in HC) correlated with decreased overall connectivity within the DMN. Similarly, Shi et al. [80] reported alterations of the DMN, including decreased functional connectivity strength in bilateral posterior cingulate

cortex, precuneus, bilateral prefrontal cortex, while increased in right posterior central gyrus, left thalamus, and left temporal lobe.

In their 2021 study, Li et al. found no significant differences in the DMN's functional connectivity between treatment-naïve patients and healthy controls, suggesting that previous abnormalities noted might be more related to medication effects rather than inherent to MDD itself. In a systematic review of 2022 by Runia et al. [81], functional connectivity within the DMN was generally decreased in treatment-resistant depression. They have also found hyperactivity in some DMN regions, which could be explained by different cellular mechanisms underlying long-range functional connectivity and local neuronal activity. However, the 2020 meta-analysis by Tozzi and Williams [82] showed very heterogeneous findings on functional connectivity within the DMN in depressed patients. These diverse findings underscore the complexity of DMN connectivity in MDD, challenging the traditional understanding that DMN connectivity is increased in MDD patients. Variations in study methodologies, symptomatology, ethnic backgrounds, and timing likely contribute to these heterogeneous results.

As previously mentioned, in the present study, clustering coefficient demonstrated significant classification capabilities, characterized by high accuracy, specificity, and sensitivity. The collaborative pursuit of classification biomarkers for mental health conditions like MDD is essential. In a related study [83] using Multivariate Pattern Analysis (MVPA), two samples of MDD patients and HCs were analyzed, achieving classification rates of 91.9% and 86.4% respectively. In this case, the findings were based on whole-brain functional connectivity. In our study, full functional connectivity matrices also had high specificity and sensitivity like as clustering coefficient.

Another research effort [84] identified 20 functional connectivities through a sparse machine learning algorithm, achieving an accuracy of 83.0%, with similar sensitivity and specificity. This study had relatively big sample sizes of MDD patients and HCs ($n = 100$ each), which is crucial for the validity of classification algorithms. In 2018, Geng et al. [85] utilized whole brain connectivity measures with various classifiers, achieving the highest performance using spectral Dynamic Causal Modeling (spDCM), which provided an accuracy of 91.30% with 19 effective connection features.

In conclusion, our study contributes to the growing evidence of the potential development of reliable diagnostic, differential diagnostic, and therapeutic biomarkers based on network measures derived from resting state fMRI functional connectivity analysis. Our findings suggest that the approach based on diagnostics of macroscopic network measures estimated by the consensus network can be very effective for revealing peculiarities of organization of functional brain networks in various psychiatric diseases and can serve as an effective method for searching for network-based biomarkers of brain diseases. For MDD patients, we have shown that clustering coefficient might be such an exemplar measure as it achieved the highest classification accuracy as well.

However, we should admit that our study suffers from several limitations. First, the sample size although bigger than many previous single site studies might not be large enough to detect smaller effects. In addition, depressed patients have been on stable antidepressant medication which might have influenced our results. The classification analysis is based on the whole sample of MDD patients and no test in an independent group has been performed.

Conclusion

Using network theory and a consensus network approach, we identified and investigated disruptions in the functional brain network segregation in patients with major depressive disorder. At the macroscale level, this was reflected in higher clustering coefficient and node strength in healthy controls, as well as differences in correspondence with large-scale brain networks. The central executive network (CEN) and the salience network (SN) are predominant in healthy controls, whereas MDD patients show greater overlap with the default mode network (DMN). No differences in network efficiency measures were found, suggesting that there are no disparities in brain network integration between the HC and MDD groups. The clustering coefficient was also found to be an effective diagnostic biomarker for MDD, resulting in a classification F1-score of 0.9 with LDA classifier. Optimal community structure analysis allowed us to examine differences in network clusters between the HC and MDD groups in more detail, at the mesoscale level. It revealed common and unique functional connections in the main clusters that distinguish the groups under consideration. In summary, we can conclude that analyzing the network first at the macroscale level and then moving to a more detailed analysis at the mesoscale level allows one to effectively overcome the main problems encountered when dealing with functional networks — large intersubject variability and the multiple comparisons problem at the network level.

Funding

V.S.K., S.A.K., and A.E.H. were supported by the Russian Science Foundation (Grant 23-71-30010) in the part of the network analysis. G.Z., R.P., S.K., M.M., and D.S. were supported by Strategic Research and Innovation Program for the Development of MU - PLOVDIV– (SRIPD-MUP), European Union – NextGenerationEU in the part of experimental works.

CRediT authorship contribution statement

Vladimir S. Khorev: Formal analysis, Investigation, Software, Writing – original draft. **Semen A. Kurkin:** Conceptualization, Investigation, Methodology, Project administration, Software, Visualization, Writing – original draft. **Gabriella Zlateva:** Data curation, Investigation, Validation, Writing – review & editing. **Rositsa Paunova:** Data curation, Investigation, Methodology, Resources, Writing – review & editing. **Sevdalina Kandilarova:** Conceptualization, Data curation, Investigation, Writing – review & editing,. **Michael Maes:** Conceptualization, Formal analysis, Funding acquisition, Investigation, Methodology, Writing – review & editing. **Drozdstoy Stoyanov:** Conceptualization, Data curation, Funding acquisition, Investigation, Methodology, Resources, Supervision, Validation, Visualization, Writing – original draft. **Alexander E. Hramov:** Conceptualization, Formal analysis, Funding acquisition, Methodology, Project administration, Resources, Supervision, Writing – review & editing,.

Declaration of competing interest

The authors declare that they have no known competing financial interests or personal relationships that could have appeared to influence the work reported in this paper.

Data availability

Data will be made available on request.

Appendix A. Supplementary information

There are three supplementary files:

- SupplementaryS1 file, which contains information about the nodes from the AAL3 atlas used in the research.
- SupplementaryS2 file, which contains the lists of nodes (brain regions) for the considered large-scale brain networks.
- SupplementaryS3 file containing information about the three largest clusters obtained from the optimal community structure analysis and their constituent connections.

Supplementary material related to this article can be found online at https://doi.org/10.1016/j.chaos.2024.115566.

References

[1] Power JD, Cohen AL, Nelson SM, Wig GS, Barnes KA, Church JA, Vogel AC, Laumann TO, Miezin FM, Schlaggar BL, et al. Functional network organization of the human brain. Neuron 2011;72(4):665–78.

[2] Hramov AE, Frolov NS, Maksimenko VA, Kurkin SA, Kazantsev VB, Pisarchik AN. Functional networks of the brain: from connectivity restoration to dynamic integration. Phys-Usp 2021;64(6):584.

[3] Boccaletti S, Latora V, Moreno Y, Chavez M, Hwang D-U. Complex networks: Structure and dynamics. Phys Rep 2006;424(4–5):175–308.

[4] Zanin M, Papo D, Sousa PA, Menasalvas E, Nicchi A, Kubik E, Boccaletti S. Combining complex networks and data mining: why and how. Phys Rep 2016;635:1–44.

[5] Perovnik M, Rus T, Schindlbeck KA, Eidelberg D. Functional brain networks in the evaluation of patients with neurodegenerative disorders. Nat Rev Neurol 2023;19(2):73–90.

[6] Bassett DS, Sporns O. Network neuroscience. Nature Neurosci 2017;20(3):353–64.

[7] Kim J, Wozniak JR, Mueller BA, Pan W. Testing group differences in brain functional connectivity: using correlations or partial correlations? Brain Connect 2015;5(4):214–31.

[8] Zalesky A, Fornito A, Bullmore ET. Network-based statistic: identifying differences in brain networks. Neuroimage 2010;53(4):1197–207.

[9] Caznok Silveira AC, Antunes ASLM, Athié MCP, da Silva BF, Ribeiro dos Santos JV, Canateli C, Fontoura MA, Pinto A, Pimentel-Silva LR, Avansini SH, et al. Between neurons and networks: investigating mesoscale brain connectivity in neurological and psychiatric disorders. Front Neurosci 2024;18:1340345.

[10] Maksimenko VA, Lüttjohann A, Makarov VV, Goremyko MV, Koronovskii AA, Nedaivozov V, Runnova AE, van Luijtelaar G, Hramov AE, Boccaletti S. Macroscopic and microscopic spectral properties of brain networks during local and global synchronization. Phys Rev E 2017;96(1):012316.

[11] Sporns O. Connectome networks: from cells to systems. Micro Meso Macro Connect Brain 2016;107–27.

[12] Mohr H, Wolfensteller U, Betzel RF, Mišić B, Sporns O, Richiardi J, Ruge H. Integration and segregation of large-scale brain networks during short-term task automatization. Nat Commun 2016;7(1):13217.

[13] Cohen JR, D'Esposito M. The segregation and integration of distinct brain networks and their relationship to cognition. J Neurosci 2016;36(48):12083–94.

[14] Wang R, Liu M, Cheng X, Wu Y, Hildebrandt A, Zhou C. Segregation, integration, and balance of large-scale resting brain networks configure different cognitive abilities. Proc Natl Acad Sci 2021;118(23):e2022288118.

[15] Pisarchik AN, Andreev AV, Kurkin SA, Stoyanov D, Badarin AA, Paunova R, Hramov AE. Topology switching during window thresholding fMRI-based functional networks of patients with major depressive disorder: Consensus network approach. Chaos 2023;33(9).

[16] GBD 2019 Mental Disorders Collaborators, et al. Global, regional, and national burden of 12 mental disorders in 204 countries and territories, 1990–2019: a systematic analysis for the Global Burden of Disease Study 2019. Lancet Psychiatry 2022;9(2):137–50.

[17] Perez DL, Aybek S, Popkirov S, Kozlowska K, Stephen CD, Anderson J, Shura R, Ducharme S, Carson A, Hallett M, et al. A review and expert opinion on the neuropsychiatric assessment of motor functional neurological disorders. J. Neuropsychiatry Clin. Neurosci. 2021;33(1):14–26.

[18] GBD Collaborators, et al. Global, regional, and national incidence, prevalence, and years lived with disability for 354 diseases and injuries for 195 countries and territories, 1990–2017: a systematic analysis for the Global Burden of Disease Study 2017. Glob. Burd. Dis. Study 2018.

[19] Malhi GS, Mann JJ. Depression. Lancet 2018;392(10161):2299–312.

[20] Burcusa SL, Iacono WG. Risk for recurrence in depression. Clin Psychol Rev 2007;27(8):959–85.

[21] Undurraga J, Baldessarini RJ. Randomized, placebo-controlled trials of antidepressants for acute major depression: thirty-year meta-analytic review. Neuropsychopharmacology 2012;37(4):851–64.

[22] Cipriani A, Furukawa TA, Salanti G, Chaimani A, Atkinson LZ, Ogawa Y, Leucht S, Ruhe HG, Turner EH, Higgins JP, et al. Comparative efficacy and acceptability of 21 antidepressant drugs for the acute treatment of adults with major depressive disorder: a systematic review and network meta-analysis. Lancet 2018;391(10128):1357–66.

[23] Krishnan V, Nestler EJ. Linking molecules to mood: new insight into the biology of depression. Am J Psychiatry 2010;167(11):1305–20.

[24] Price JL, Drevets WC. Neural circuits underlying the pathophysiology of mood disorders. Trends Cogn Sci 2012;16(1):61–71.

[25] Miller AH, Raison CL. The role of inflammation in depression: from evolutionary imperative to modern treatment target. Nat Rev Immunol 2016;16(1):22–34.

[26] Krystal J, Sanacora G, Blumberg H, Anand A, Charney D, Marek G, Epperson C, Goddard A, Mason G. Glutamate and GABA systems as targets for novel antidepressant and mood-stabilizing treatments. Mol Psychiatry 2002;7(1):S71–80.

[27] Brunoni AR, Lopes M, Fregni F. A systematic review and meta-analysis of clinical studies on major depression and BDNF levels: implications for the role of neuroplasticity in depression. Int J Neuropsychopharmacol 2008;11(8):1169–80.

[28] Black C, Bot M, Scheffer P, Penninx B. Oxidative stress in major depressive and anxiety disorders, and the association with antidepressant use; results from a large adult cohort. Psychol Med 2017;47(5):936–48.

[29] Di Nicola V, Stoyanov D, Di Nicola V, Stoyanov D. Psychiatric nosology revisited: At the crossroads of psychology and medicine. In: Psychiatry in crisis at the crossroads of social sciences, the humanities, and neuroscience. Springer; 2021, p. 31–41.

[30] Kaiser RH, Andrews-Hanna JR, Wager TD, Pizzagalli DA. Large-scale network dysfunction in major depressive disorder: a meta-analysis of resting-state functional connectivity. JAMA Psychiatry 2015;72(6):603–11.

[31] Parkes L, Satterthwaite TD, Bassett DS. Towards precise resting-state fMRI biomarkers in psychiatry: synthesizing developments in transdiagnostic research, dimensional models of psychopathology, and normative neurodevelopment. Curr Opin Neurobiol 2020;65:120–8.

[32] Seitzman BA, Snyder AZ, Leuthardt EC, Shimony JS. The state of resting state networks. Top Magn Reson Imaging 2019;28(4):189–96.

[33] Hugdahl K, Raichle ME, Mitra A, Specht K. On the existence of a generalized non-specific task-dependent network. Front Hum Neurosci 2015;9. http://dx.doi.org/10.3389/fnhum.2015.00430.

[34] Todeva-Radneva A, Kandilarova S, Paunova R, Stoyanov D, Zdravkova T, Sladky R. Functional connectivity of the anterior cingulate cortex and the right anterior insula differentiates between major depressive disorder, bipolar disorder and healthy controls. Biomedicines 2023;11(6):1608. http://dx.doi.org/10.3390/biomedicines11061608.

[35] Zhou Z, Gao Y, Bao W, Liang K, Cao L, Tang M, Li H, Hu X, Zhang L, Sun H, Roberts N, Gong Q, Huang X. Distinctive intrinsic functional connectivity alterations of anterior cingulate cortex subdivisions in major depressive disorder: A systematic review and meta-analysis. Neurosci Biobehav Rev 2024;159:105583.

[36] Dai P, Zhou X, Xiong T, Ou Y, Chen Z, Zou B, Li W, Huang Z. Altered effective connectivity among the cerebellum and cerebrum in patients with major depressive disorder using multisite resting-state fMRI. Cerebellum 2022;22(5):781–9.

[37] Ni S, Gao S, Ling C, Jiang J, Wu F, Peng T, Sun J, Zhang N, Xu X. Altered brain regional homogeneity is associated with cognitive dysfunction in first-episode drug-naive major depressive disorder: A resting-state fMRI study. J Affect Disord 2023;343:102–8.

[38] Yu AH, Gao QL, Deng ZY, Dang Y, Yan CG, Chen ZZ, Li F, Zhao SY, Liu Y, Bo QJ. Common and unique alterations of functional connectivity in major depressive disorder and bipolar disorder. Bipolar Disord 2023;25(4):289–300.

[39] Kang L, Zhang A, Sun N, Liu P, Yang C, Li G, Liu Z, Wang Y, Zhang K. Functional connectivity between the thalamus and the primary somatosensory cortex in major depressive disorder: a resting-state fMRI study. BMC Psychiatry 2018;18(1).

[40] Kaiser RH, Andrews-Hanna JR, Wager TD, Pizzagalli DA. Large-scale network dysfunction in major depressive disorder: A meta-analysis of resting-state functional connectivity. JAMA Psychiatry 2015;72(6):603.

[41] Yan C-G, Chen X, Li L, Castellanos FX, Bai T-J, Bo Q-J, Cao J, Chen G-M, Chen N-X, Chen W, Cheng C, Cheng Y-Q, Cui X-L, Duan J, Fang Y-R, Gong Q-Y, Guo W-B, Hou Z-H, Hu L, Kuang L, Li F, Li K-M, Li T, Liu Y-S, Liu Z-N, Long Y-C, Luo Q-H, Meng H-Q, Peng D-H, Qiu H-T, Qiu J, Shen Y-D, Shi Y-S, Wang C-Y, Wang F, Wang K, Wang L, Wang X, Wang Y, Wu X-P, Wu X-R, Xie C-M, Xie G-R, Xie H-Y, Xie P, Xu X-F, Yang H, Yang J, Yao J-S, Yao S-Q, Yin Y-Y, Yuan Y-G, Zhang A-X, Zhang H, Zhang K-R, Zhang L, Zhang Z-J, Zhou R-B, Zhou Y-T, Zhu J-J, Zou C-J, Si T-M, Zuo X-N, Zhao J-P, Zang Y-F. Reduced default mode network functional connectivity in patients with recurrent major depressive disorder. Proc Natl Acad Sci 2019;116(18):9078–83.

[42] Stoyanov D, Khorev V, Paunova R, Kandilarova S, Simeonova D, Badarin A, Hramov A, Kurkin S. Resting-state functional connectivity impairment in patients with major depressive episode. Int J Environ Res Public Health 2022;19(21):14045.

[43] Pitsik EN, Maximenko VA, Kurkin SA, Sergeev AP, Stoyanov D, Paunova R, Kandilarova S, Simeonova D, Hramov AE. The topology of fMRI-based networks defines the performance of a graph neural network for the classification of patients with major depressive disorder. Chaos Solitons Fractals 2023;167:113041.

[44] Andreev AV, Kurkin SA, Stoyanov D, Badarin AA, Paunova R, Hramov AE. Toward interpretability of machine learning methods for the classification of patients with major depressive disorder based on functional network measures. Chaos 2023;33(6).

[45] Sheehan DV, Lecrubier Y, Sheehan KH, Amorim P, Janavs J, Weiller E, Hergueta T, Baker R, Dunbar GC, et al. The Mini-International Neuropsychiatric Interview (MINI): the development and validation of a structured diagnostic psychiatric interview for DSM-IV and ICD-10. J Clin Psychiatry 1998;59(20):22–33.

[46] Müller MJ, Himmerich H, Kienzle B, Szegedi A. Differentiating moderate and severe depression using the Montgomery–Åsberg depression rating scale (MADRS). J Affect Disord 2003;77(3):255–60.

[47] Montgomery SA, Åsberg M. A new depression scale designed to be sensitive to change. Br J Psychiatry 1979;134(4):382–9.

[48] Stoyanov D, Kandilarova S, Aryutova K, Paunova R, Todeva-Radneva A, Latypova A, Kherif F. Multivariate analysis of structural and functional neuroimaging can inform psychiatric differential diagnosis. Diagnostics 2020;11(1):19.
[49] Rolls ET, Huang C-C, Lin C-P, Feng J, Joliot M. Automated anatomical labelling atlas 3. Neuroimage 2020;206:116189.
[50] Stanley ML, Moussa MN, Paolini BM, Lyday RG, Burdette JH, Laurienti PJ. Defining nodes in complex brain networks. Front. Comput. Neurosci. 2013;7:169.
[51] Stoyanov D, Khorev V, Paunova R, Kandilarova S, Simeonova D, Badarin A, Hramov A, Kurkin S. Resting-state functional connectivity impairment in patients with major depressive episode. Int J Environ Res Public Health 2022;19(21):14045.
[52] Rubinov M, Sporns O. Weight-conserving characterization of complex functional brain networks. Neuroimage 2011;56(4):2068–79.
[53] Brandes U. A faster algorithm for betweenness centrality. J Math Sociol 2001;25(2):163–77.
[54] Caeyenberghs K, Verhelst H, Clemente A, Wilson PH. Mapping the functional connectome in traumatic brain injury: What can graph metrics tell us? Neuroimage 2017;160:113–23.
[55] Newman ME. The mathematics of networks. New Palgrave Encycl Econ 2008;2(2008):1–12.
[56] Costantini G, Perugini M. Generalization of clustering coefficients to signed correlation networks. PLoS One 2014;9(2):e88669.
[57] Latora V, Marchiori M. Efficient behavior of small-world networks. Phys Rev Lett 2001;87(19):198701.
[58] Reichardt J, Bornholdt S. Statistical mechanics of community detection. Phys Rev E 2006;74(1):016110.
[59] Rubinov M, Sporns O. Complex network measures of brain connectivity: uses and interpretations. Neuroimage 2010;52(3):1059–69.
[60] Oliver I, Hlinka J, Kopal J, Davidsen J. Quantifying the variability in resting-state networks. Entropy 2019;21(9):882.
[61] Manoliu A, Meng C, Brandl F, Doll A, Tahmasian M, Scherr M, Schwerthöffer D, Zimmer C, Förstl H, Bäuml J, et al. Insular dysfunction within the salience network is associated with severity of symptoms and aberrant inter-network connectivity in major depressive disorder. Front Hum Neurosci 2014;7:930.
[62] Alves PN, Forkel SJ, Corbetta M, Thiebaut de Schotten M. The subcortical and neurochemical organization of the ventral and dorsal attention networks. Commun Biol 2022;5(1):1343.
[63] Chen Q, Baran TM, Turnbull A, Zhang Z, Rebok GW, Lin FV. Increased segregation of structural brain networks underpins enhanced broad cognitive abilities of cognitive training. Hum Brain Mapp 2021;42(10):3202–15.
[64] Lohmann G, Margulies DS, Horstmann A, Pleger B, Lepsien J, Goldhahn D, Schloegl H, Stumvoll M, Villringer A, Turner R. Eigenvector centrality mapping for analyzing connectivity patterns in fMRI data of the human brain. PLoS One 2010;5(4):e10232.
[65] Sheline YI, Barch DM, Price JL, Rundle MM, Vaishnavi SN, Snyder AZ, Mintun MA, Wang S, Coalson RS, Raichle ME. The default mode network and self-referential processes in depression. Proc Natl Acad Sci 2009;106(6):1942–7.
[66] Jacob Y, Morris LS, Huang K-H, Schneider M, Rutter S, Verma G, Murrough JW, Balchandani P. Neural correlates of rumination in major depressive disorder: A brain network analysis. NeuroImage Clin 2020;25:102142.
[67] Huang S-S, Yu Y-H, Chen H-H, Hung C-C, Wang Y-T, Chang CH, Peng S-J, Kuo P-H. Functional connectivity analysis on electroencephalography signals reveals potential biomarkers for treatment response in major depression. BMC Psychiatry 2023;23(1).
[68] Jacob Y, Morris LS, Verma G, Rutter SB, Balchandani P, Murrough JW. Altered hippocampus and amygdala subregion connectome hierarchy in major depressive disorder. Transl Psychiatry 2022;12(1):209.
[69] Liu J, Zhu Q, Zhu L, Yang Y, Zhang Y, Liu X, Zhang L, Jia Y, Peng Q, Wang J, et al. Altered brain network in first-episode, drug-naive patients with major depressive disorder. J Affect Disord 2022;297:1–7.
[70] Xia M, Womer FY, Chang M, Zhu Y, Zhou Q, Edmiston EK, Jiang X, Wei S, Duan J, Xu K, et al. Shared and distinct functional architectures of brain networks across psychiatric disorders. Schizophr Bull 2019;45(2):450–63.
[71] Wu B, Chen Y, Long X, Cao Y, Xie H, Wang X, Roberts N, Gong Q, Jia Z. Altered single-subject gray matter structural networks in first-episode drug-naïve adolescent major depressive disorder. Psychiatry Res 2023;329:115557.
[72] Borchardt V, Lord AR, Li M, van der Meer J, Heinze H-J, Bogerts B, Breakspear M, Walter M. Preprocessing strategy influences graph-based exploration of altered functional networks in major depression. Hum Brain Mapp 2016;37(4):1422–42.
[73] Lord A, Horn D, Breakspear M, Walter M. Changes in community structure of resting state functional connectivity in unipolar depression. USA: Public Library of Science San Francisco; 2012.
[74] Peng D, Shi F, Shen T, Peng Z, Zhang C, Liu X, Qiu M, Liu J, Jiang K, Fang Y, et al. Altered brain network modules induce helplessness in major depressive disorder. J Affect Disord 2014;168:21–9.
[75] He H, Yu Q, Du Y, Vergara V, Victor TA, Drevets WC, Savitz JB, Jiang T, Sui J, Calhoun VD. Resting-state functional network connectivity in prefrontal regions differs between unmedicated patients with bipolar and major depressive disorders. J Affect Disord 2016;190:483–93.
[76] Dai Y-R, Wu Y-K, Chen X, Zeng Y-W, Li K, Li J-T, Su Y-A, Zhu L-L, Yan C-G, Si T-M. Eight-week antidepressant treatment changes intrinsic functional brain topology in first-episode drug-naïve patients with major depressive disorder. J Affect Disord 2023;329:225–34.
[77] Chu S-H, Parhi KK, Westlund Schreiner M, Lenglet C, Mueller BA, Klimes-Dougan B, Cullen KR. Effect of SSRIs on resting-state functional brain networks in adolescents with major depressive disorder. J Clin Med 2021;10(19):4322.
[78] Mulders PC, van Eijndhoven PF, Schene AH, Beckmann CF, Tendolkar I. Resting-state functional connectivity in major depressive disorder: a review. Neurosci Biobehav Rev 2015;56:330–44.
[79] Yan C-G, Chen X, Li L, Castellanos FX, Bai T-J, Bo Q-J, Cao J, Chen G-M, Chen N-X, Chen W, et al. Reduced default mode network functional connectivity in patients with recurrent major depressive disorder. Proc Natl Acad Sci 2019;116(18):9078–83.
[80] Shi Y, Li J, Feng Z, Xie H, Duan J, Chen F, Yang H. Abnormal functional connectivity strength in first-episode, drug-naive adult patients with major depressive disorder. Prog Neuropsychopharmacol Biol Psych 2020;97:109759.
[81] Runia N, Yücel DE, Lok A, de Jong K, Denys DA, van Wingen GA, Bergfeld IO. The neurobiology of treatment-resistant depression: a systematic review of neuroimaging studies. Neurosci Biobehav Rev 2022;132:433–48.
[82] Tozzi L, Zhang X, Chesnut M, Holt-Gosselin B, Ramirez CA, Williams LM. Reduced functional connectivity of default mode network subsystems in depression: meta-analytic evidence and relationship with trait rumination. NeuroImage Clin 2021;30:102570.
[83] Zhong X, Shi H, Ming Q, Dong D, Zhang X, Zeng L-L, Yao S. Whole-brain resting-state functional connectivity identified major depressive disorder: a multivariate pattern analysis in two independent samples. J Affect Disord 2017;218:346–52.
[84] Ichikawa N, Okamoto Y, Okada G, Lisi G, Yahata N, Morimoto J, Kawato M, Matsuo K, Yamagata H, Watanabe Y, et al. Neuroimaging biomarker of major depressive disorder. Eur Psychiatry 2016;33(S1):S492–3.
[85] Geng X, Xu J, Liu B, Shi Y. Multivariate classification of major depressive disorder using the effective connectivity and functional connectivity. Front Neurosci 2018;12:38.